Two Poplar Glycosyltransferase Genes, *PdGATL1.1* and *PdGATL1.2*, Are Functional Orthologs to *PARVUS/AtGATL1* in *Arabidopsis*

Yingzhen Kong[a,b,2], Gongke Zhou[a,b,2,3], Utku Avci[a,b], Xiaogang Gu[a], Chelsea Jones[a], Yanbin Yin[b,c], Ying Xu[b,c] and Michael G. Hahn[a,b,1]

a Complex Carbohydrate Research Center, The University of Georgia, 315 Riverbend Road, Athens, GA 30602, USA
b BioEnergy Science Center, The University of Georgia, 315 Riverbend Road, Athens, GA 30602, USA
c Computational System Biology Lab, Dept. of Biochemistry and Molecular Biology, and Institute of Bioinformatics, The University of Georgia, Athens, GA 30602, USA

ABSTRACT   **Several genes in *Arabidopsis*, including *PARVUS/AtGATL1*, have been implicated in xylan synthesis. However, the biosynthesis of xylan in woody plants, where this polysaccharide is a major component of wood, is poorly understood. Here, we characterize two *Populus* genes, *PdGATL1.1* and *PdGATL1.2*, the closest orthologs to the *Arabidopsis PARVUS/ GATL1* gene, with respect to their gene expression in poplar, their sub-cellular localization, and their ability to complement the *parvus* mutation in *Arabidopsis*. Overexpression of the two poplar genes in the *parvus* mutant rescued most of the defects caused by the *parvus* mutation, including morphological changes, collapsed xylem, and altered cell wall monosaccharide composition. Quantitative RT–PCR showed that *PdGATL1.1* is expressed most strongly in developing xylem of poplar. In contrast, *PdGATL1.2* is expressed much more uniformly in leaf, shoot tip, cortex, phloem, and xylem, and the transcript level of *PdGATL1.2* is much lower than that of *PdGATL1.1* in all tissues examined. Sub-cellular localization experiments showed that these two proteins are localized to both ER and Golgi in comparison with marker proteins resident to these sub-cellular compartments. Our data indicate that PdGATL1.1 and PdGATL1.2 are functional orthologs of PARVUS/ GATL1 and can play a role in xylan synthesis, but may also have role(s) in the synthesis of other wall polymers.**

Key words: *Arabidopsis thaliana*; poplar; xylan; glycosyltransferase.

INTRODUCTION

Xylans are polymers with a linear backbone composed entirely of β-D-Xyl residues connected through (1→4)-linkages that are partially acetylated and sometimes substituted with glucuronic acid and 4-*O*-methyl glucuronic acid (glucuronoxylan, GX), arabinose (arabinoxylan), or a combination of acidic and neutral sugars (glucuronoarabinoxylan). Glucuronoxylans are major components of the secondary walls of dicots and are second only to cellulose in polysaccharide abundance in plant biomass, composing, for example, 23% of the dry weight of poplar wood (Simson and Timell, 1978). An understanding of GX biosynthesis has implications in economically important industries including biofuel production, where optimization of the plant cell wall composition to overcome biomass recalcitrance is a major goal of research (Bevan and Franssen, 2006).

GX has typically been viewed as a polysaccharide whose synthesis requires a xylan synthase for backbone formation and one or more glycosyltransferases for the addition of side chains. A number of glycosyltransferases have been identified

that appear to be involved in xylan synthesis in *Arabidopsis*, including IRX8/AtGAUT12 (Persson et al., 2007; Peña et al., 2007), IRX9 (Peña et al., 2007), IRX7/FRA8 (Peña et al., 2007; Brown et al., 2007), PARVUS/AtGATL1 (Brown et al., 2007; Lee et al., 2007), IRX14 (Brown et al., 2007), IRX10, and IRX10-L (Brown et al., 2007; Wu et al., 2009). Plants carrying mutations in one or more of the genes encoding these proteins show similar phenotypes, including dwarfism, collapsed xylem,

and decreased xylan and xylose content. However, these gly-cosyltransferases appear to be involved in different aspects of the biosynthetic process. For example, IRX9, IRX14, IRX10, and IRX10-L (Peña et al., 2007; Brown et al., 2007; Wu et al., 2009; Brown et al., 2009) appear to be involved in elongation of the xylan backbone, whereas IRX7, IRX8/AtGAUT12, and PARVUS/AtGATL1 (Persson et al., 2007; Peña et al., 2007; Lee et al., 2007) appear to be involved in the synthesis of a galac-turonic acid-containing tetramer that is located at the reduc-ing end of xylan. This reducing-terminal tetrasaccharide appears to play an important role during xylan synthesis, al-though it is not known whether this oligosaccharide acts as a primer or a terminator (York and O'Neill, 2008). The exact role(s) of each of these proteins in the synthesis of xylan remain unclear, in part, due to the absence of functional *in vitro* assays of enzyme activity. Two of these proteins, IRX8/AtGAUT12 and PARVUS/AtGATL1, are related by sequence to a functionally characterized galacturonosyltransferase (AtGAUT1) (Sterling et al., 2006), suggesting that they might be involved in the syn-thesis of the xylan-terminal tetrasaccharide via the addition of an α-linked GalA residue to the growing tetrasaccharide (Pers-son et al., 2007; Peña et al., 2007). Another possibility is that these two proteins are involved in the synthesis of a structure to which the reducing end xylan oligosaccharide is attached, for example, a specific pectic polysaccharide (Mohnen, 2008).

Despite these advances in *Arabidopsis*, little is known about the genes involved in wood formation in trees, which contain xylan as a major hemicellulosic component (Ebringerová et al., 2005). *Populus trichocarpa* has been fully sequenced and a to-tal of 45 555 gene models have been predicted (Tuskan et al., 2006). The completion of the *P. trichocarpa* genome sequence provides an opportunity to advance our knowledge of wood formation. However, the scarcity of loss-of-function mutants complicates the study of gene function in poplar. *Arabidopsis* has been suggested as a model system for the study of secondary growth because this herbaceous species, under specific growing conditions, can be induced to develop features that exhibit many of the characteristics common to secondary growth in tree species (Chaffey et al., 2002; Ko and Han, 2004).

Recent studies have shown that *PoGT43B* and *PoGT47C*, the poplar orthologs of *IRX9* and *IRX7/FRA8*, respectively, are able to rescue the xylan defects of *irx9* and *irx7/fra8* mutants in *Ara-bidopsis* (Zhou et al., 2006, 2007). These findings indicate that *PoGT43B* and *PoGT47C* are likely to be involved in xylan syn-thesis during wood formation. These results also established the feasibility of using *Arabidopsis* as a model plant in which to study the functions of poplar glycosyltransferases that par-ticipate in wood formation.

In this study, we report molecular and genetic characteriza-tion of two poplar genes, *PdGATL1.1* and *PdGATL1.2*, that are orthologous to the *Arabidopsis PARVUS/AtGATL1* gene. These two poplar genes are highly expressed in developing wood (Aspeborg et al., 2005), and are specifically up-regulated in sec-ondary wall-forming zones (Geisler-Lee et al., 2006; Mellerowicz

and Sundberg, 2008) and down-regulated during tension wood formation (Andersson-Gunnerås et al., 2006), which indicates that they may play roles in wood formation. However, the exact function(s) of the proteins encoded by these two genes are still unclear. So, in order to gain further insight into the functions of these two poplar genes, we examined their expression patterns in poplar tissues, the sub-cellular localization of the correspond-ing proteins, and their ability to complement the *parvus/gatl1* mutant in *Arabidopsis*.

RESULTS

Gene Structure and Expression Profiles of Poplar *GATL1.1* and *GATL1.2*

Two poplar genes named *GATL1.1* and *GATL1.2* were identi-fied from the *Populus trichocarpa* genome database (www.jgi.doe.gov/poplar) on the basis of their sequence sim-ilarity to the *Arabidopsis PARVUS/AtGATL1* gene (Figure 1A). The corresponding genes, *PdGATL1.1* and *PdGATL1.2*, were then cloned and sequenced from *Populus deltoides* xylem-derived cDNA. Except for the *P. trichocarpa* sequences used for generation of the phylogenetic tree, all the other sequen-ces of poplar *GATL1.1* and *GATL1.2* mentioned in this paper are from *Populus deltoides*. *PdGATL1.1* encodes a protein of 360 amino acids and *PdGATL1.2* encodes a protein of 353 amino acids. Pair-wise comparisons of the amino acid sequences showed that these two proteins are highly similar, having 93% sequence identity with each other. Further, these two poplar proteins have 82 and 81% identity, respectively, at the amino acid level with PARVUS/AtGATL1 (Figure 1B).

The expression profiles of the two genes were examined by quantitative real-time PCR using primers that were specific to each gene. Cortex, phloem, xylem, shoot tip, leaf, and root tis-sues were harvested from young *Populus deltoides* trees grown in a greenhouse. Ubiquitin was used as an internal con-trol. As indicated in Figure 2, *PdGATL1.1* and *PdGATL1.2* are expressed ubiquitously in all the tissues, though their relative ex-pression levels are very different. *PdGATL1.1* is highly expressed in xylem compared to other tissues. *PdGATL1.2* expression is highest in xylem, but overall transcript levels are more uniform in all tissues examined, except root and *PdGATL1.2* transcript levels are much lower than *PdGATL1.1* levels. For example, in xy-lem, the expression level of *PdGATL1.1* is 26 times that of *PdGATL1.2*.

PdGATL1.1 and PdGATL1.2 Are Targeted to the Secretory Pathway

Predictions about the sub-cellular localization of the PdGATL1 proteins were made by subjecting the PdGATL1 amino acid sequences to analyses using publicly available bioinformatics packages, including SOSUI, TMHMM 2.0, and PSORT (see Methods). PdGATL1.2 was predicted to have no transmem-brane domain by all programs used, and is predicted by PSORT to have a cleavable N-terminal signal peptide that directs the
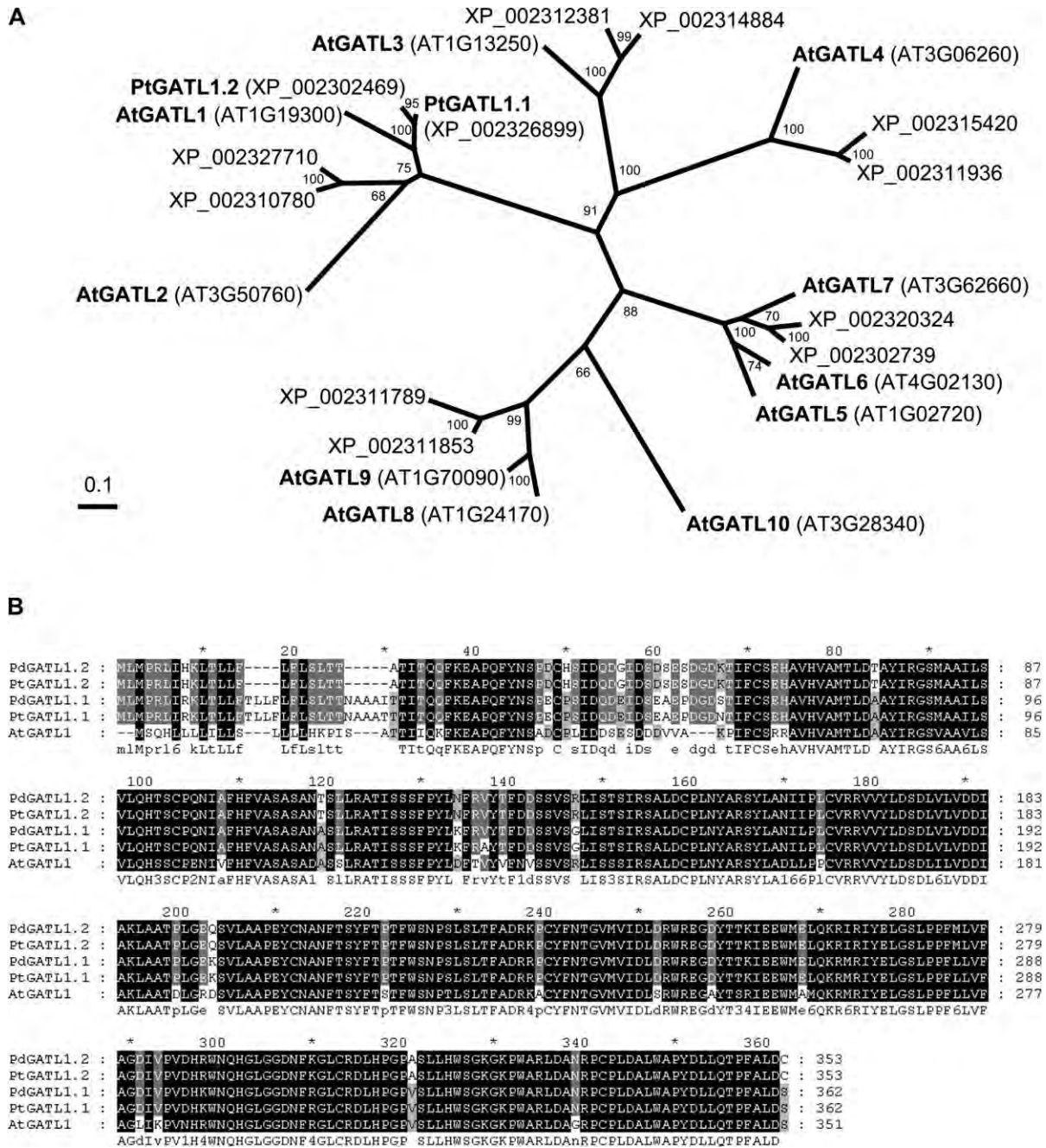
Figure 1. Phylogenetic Tree and Multiple Sequence Alignments Were Constructed from the Deduced Amino Acid Sequences of the 10-Member *Arabidopsis thaliana* GATL Family and the Orthologous Proteins from *Populus trichocarpa* and *P. deltoides*.

(A) The protein sequences from *A. thaliana* and *P. trichocarpa* were aligned using MAFFT v6.603 (Katoh et al., 2005) and the resulting alignment was used to perform maximum likelihood phylogeny reconstruction using PhyML v2.4.4 (Guindon and Gascuel, 2003). *P. trichocarpa* GATL protein sequences are identified by their NCBI RefSeq accessions (www.ncbi.nlm.nih.gov/RefSeq/).

(B) Amino acid sequence alignment of PtGATL1.1, PtGATL1.2, PdGATL1.1, PdGATL1.2, and PARVUS/AtGATL1. Gaps (marked with dashes) were introduced to maximize the sequence alignment. Identical and similar amino acid residues are shaded with black and gray, respectively.

protein into the secretory pathway. For PdGATL1.1, no consensus was found among the prediction programs used. PSORT predicts the presence of a cleavable N-terminal signal peptide that directs the protein into the secretory pathway, the same as

PdGATL1.2. But SOSUI and TMHMM 2.0 predict that PdGATL1.1 could be an integral membrane protein with one transmembrane domain. Similarly, the PARVUS/AtGATL1 protein is predicted to have a signal peptide sequence at the N-terminus by
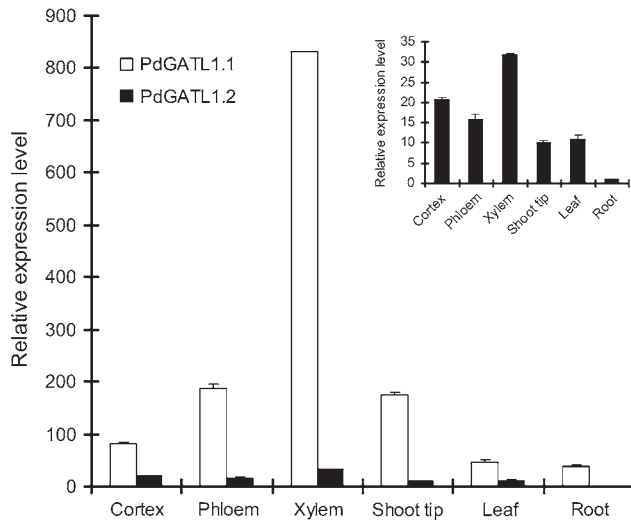
Figure 2. Expression Analysis of the *PdGATL1.1* and *PdGATL1.2* Genes by Quantitative Real-Time PCR.

Relative expression levels in all samples were normalized using ubiquitin as a constitutively expressed internal control and the *PdGATL1.2* expression levels in root are set to 1. Data are the averages ± SE of three biological replicates.

PSORT, and no transmembrane domain is predicted for this protein by TMHMM 2.0. However, SOSUI predict that PARVUS/AtGATL1 has a 23-amino acid transmembrane domain that includes the N-terminal amino acids 1 to 23. This would leave no cytosolic N-terminal domain, which would be unusual for a type II membrane. So it seems most likely that both PARVUS/AtGATL1 and PdGATL1.2 have no transmembrane domain, but rather just an N-terminal signal peptide directing the protein into the endomembrane secretory system. Considering the high amino acid similarity of PdGATL1.1 with these two proteins, it is highly likely that PdGATL1.1 also has no transmembrane domain.

The PARVUS/GATL1 protein was previously suggested to be localized in endoplasmic reticulum (ER) based on the localization of a heterologously expressed enhanced yellow fluorescence protein (EYFP)-tagged PARVUS/GATL1 recombinant protein in carrot protoplasts (Lee et al., 2007). To investigate whether PdGATL1.1 and PdGATL1.2 have the same sub-cellular localization as PARVUS/GATL1, we fused PdGATL1.1 and PdGATL1.2 with EYFP at the C-terminus and transformed the recombinant protein into *Nicotiana benthamiana* leaves. Confocal microscopy was used to determine the sub-cellular localization of recombinant PdGATL1.1 and PdGATL1.2. As shown in Figure 3B, 3E, 3H, and 3K, EYFP-tagged PdGATL1.1 and PdGATL1.2 showed both punctuate and network-like localization patterns in tobacco leaf epidermal cells. Co-localization experiments (Figure 3C, 3F, 3I, and 3L) revealed that these patterns overlap with those of both Gmct-ECFP, an enhanced cyan fluorescent protein (ECFP)-tagged Golgi marker (Saint-Jore-Dupas et al., 2006; Nelson et al., 2007), and ECFP-WAK2-HDEL, an ER marker (Nelson et al., 2007) (Figure 3A, 3D, 3G, and 3J).
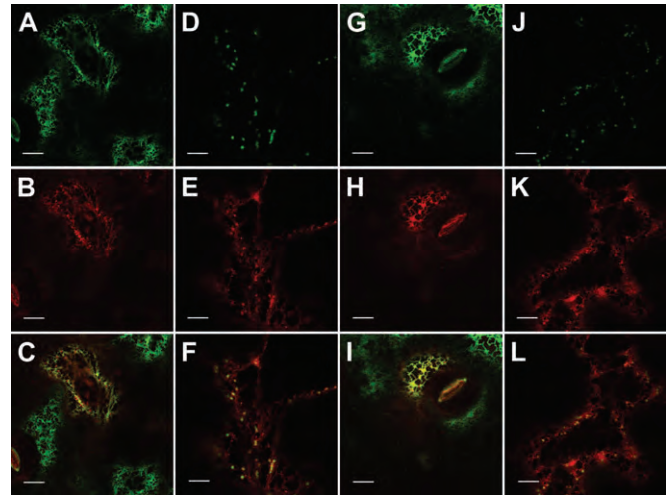

Figure 3. Sub-Cellular Localization of EYFP Tagged PdGATL1.1 and PdGATL1.2 Proteins.

EYFP-tagged PdGATL1.1 and PdGATL1.2 were transiently expressed in leaf epidermal cells of *Nicotiana benthamiana* plants, and their sub-cellular locations were examined with a laser scanning confocal microscope. Scale bars represent 20 μm.

(A–C) Tobacco leaf epidermal cells expressing both PdGATL1.1–EYFP and ECFP–WAK2–HDEL constructs. (A) localization of ECFP–WAK2–HDEL ER marker protein (green). (B) localization of PdGATL1.1–EYFP protein (red) in the same cell as in (A). (C) merged image of (A) and (B), showing co-localization of PdGATL1.1–EYFP and ECFP-WAK2-HDEL.

(D–F) Tobacco leaf epidermal cells expressing both PdGATL1.1–EYFP and Gmct–ECFP constructs. (D) Localization of Gmct–ECFP Golgi marker protein (green). (E) Localization of PdGATL1.1–EYFP protein (red) in the same cell as in (D). (F) Merged image of (D) and (E), showing co-localization of PdGATL1.1–EYFP and Gmct–ECFP.

(G–I) Tobacco leaf epidermal cells expressing both PdGATL1.2–EYFP and ECFP-WAK2-HDEL constructs. (G) Localization of ECFP–WAK2–HDEL ER marker protein (green). (H) Localization of PdGATL1.2–EYFP protein (red) in the same cell as in (G). (I) Merged image of (G) and (H), showing co-localization of PdGATL1.2–EYFP and ECFP–WAK2–HDEL.

(J–L) Tobacco leaf epidermal cells expressing both PdGATL1.2–EYFP and Gmct–ECFP constructs. (J) Localization of Gmct–ECFP Golgi marker protein (green). (K) Localization of PdGATL1.2–EYFP protein (red) in the same cell as in (J). (L) Merged image of (J) and (H), showing co-localization of PdGATL1.2–EYFP and Gmct–ECFP.

PdGATL1.1 and *PdGATL1.2* Rescue *Arabidopsis parvus/atgatl1* Mutant Phenotypes

To determine whether PdGATL1.1 and PdGATL1.2 have the same function as PARVUS/AtGATL1, we attempted to complement the *Arabidopsis parvus/gatl1* mutant with the full-length poplar genes. The open reading frames of the two *P. deltoides* genes were cloned from xylem-derived cDNA fused with the cauliflower mosaic virus (CaMV) 35S promoter, and introduced individually into a heterozygous *parvus/gatl1* mutant line of *Arabidopsis* (homozygous *parvus/gatl1* plants have very low fertility (Lao et al., 2003; Shao et al., 2004; Lee et al., 2007), necessitating the use of the heterozygous line). Transgenic lines were tested for the presence of the *PdGATL1.1* and

PdGATL1.2 transgenes in a homozygous *parvus/gatl1* background. Using poplar gene-specific primers for transgene amplification, poplar mRNA expression in the transgenic *Arabidopsis* lines was confirmed by RT–PCR (Figure 4B and 4C). The absence of *PARVUS/AtGATL1* gene expression in the transgenic lines was also confirmed using primers specific to the wild-type (w.t.) *Arabidopsis* gene (Figure 4B and 4C).

Homozygous *parvus/gatl1* mutants show dark-green leaves, reduced plant stature, reduced size of all organs, including leaves, floral organs, and fruits, and reduced fertility (Lao et al., 2003; Shao et al., 2004; Lee et al., 2007). Expression of either *PdGATL1.1* or *PdGATL1.2* in the *parvus/gatl1* mutant rescued the morphological defects in the mutant. Indeed, the
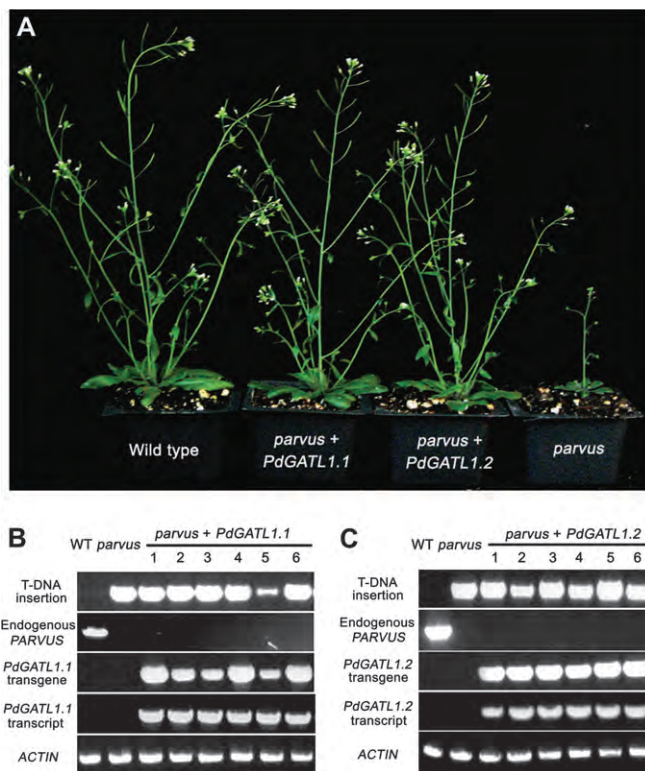

Figure 4. Restoration of Plant Size in *Arabidopsis parvus* Plants by Overexpression of the Poplar *PdGATL1.1* and *PdGATL1.2* Genes, Respectively.

The results shown are representative of six independent transgenic *Arabidopsis* lines. All transgenic plants were confirmed to have a homozygous *parvus* background by PCR detection of the T-DNA insertion and absence of an endogenous *PARVUS* gene compared with the w.t. (upper two panels in (B) and (C)).
(A) The *parvus* mutant (right) has a short inflorescence stem and a small rosette size, and overexpression of *PdGATL1.1* and *PdGATL1.2*, respectively, in *parvus* plants (middle) restored the stem height and rosette size to those of the w.t. (left).
(B) PCR detection of the *PdGATL1.1* transgene and its transcript in the transgenic *parvus* plants. The expression of the *ACTIN* gene was used as an internal control.
(C) PCR detection of the *PdGATL1.2* transgene and its transcript in the transgenic *parvus* plants. The expression of the *ACTIN* gene was used as an internal control. WT, wild-type.

morphology of the complemented plants is indistinguishable from that of w.t. *Arabidopsis* plants (Figure 4A).

The *parvus/gatl1* mutant also exhibits collapsed xylem vessels and thinner secondary cell walls, which are largely due to defects in xylan synthesis (Brown et al., 2007; Lee et al., 2007). In *parvus/gatl1* mutants, the xylose content is decreased by about 47% compared to w.t. (Lee et al., 2007). To demonstrate whether the morphological complementation by *PdGATL1.1* and *PdGATL1.2* could be correlated with a rescue of xylan synthesis, xylem morphology and xylan immunolocalization were examined in the transgenic plants and cell wall glycosyl residue compositions of the transgenic plants were determined. As shown in Figure 5, the shapes of xylem vessels in either the *PdGATL1.1* or *PdGATL1.2* complemented plants were essentially indistinguishable from those of xylem vessels in w.t. plants. Cell wall monosaccharide analysis revealed that overexpression of either *PdGATL1.1* or *PdGATL1.2* in a *parvus/gatl1* background restored the level of xylose to 86 and 80% of w.t. levels, respectively (Figure 6).

Immunolocalization of xylan using the xylan-directed monoclonal antibodies LM10 and LM11 was done to further investigate whether the increased xylose content and the complemented phenotype in the transgenic plants correlate with the rescue of xylan synthesis in secondary cell walls. LM10 has been reported to bind to 4-*O*-methylglucuronoxylan, but not to arabinoxylan and glucuronoarabinoxylan, whereas LM11 interacts with both 4-*O*-methylglucuronoxylan and
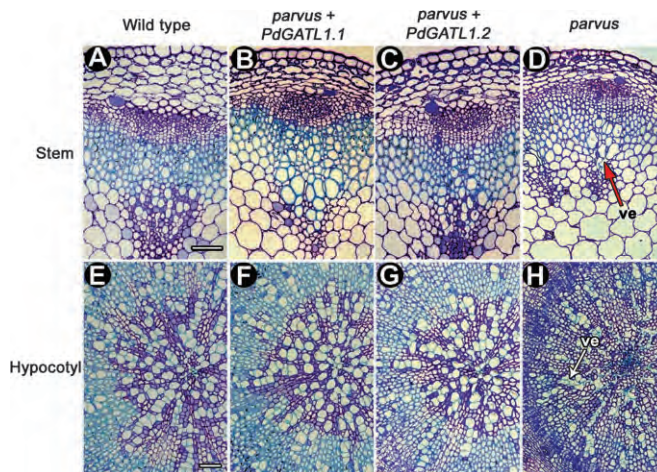

Figure 5. Restoration of Secondary Wall Thickness of Vessels in the Transgenic *Arabidopsis parvus* Plants Overexpressing the Poplar *PdGATL1.1* and *PdGATL1.2* Genes, Respectively.

Stems and hypocotyls of 8-week-old plants were sectioned (250 nm thick) and stained with toluidine blue for examination of vessels. Arrows indicate collapsed vessels. ve, vessel. Images for each tissue are taken at the same magnification. Bars = 50 μm.
(A–D) Transverse sections taken from the base of stems of w.t., *PdGATL1.1*-complemented *parvus*, *PdGATL1.2*-complemented *parvus*, and *parvus*, respectively.
(E–H) Transverse sections taken from hypocotyls of w.t., *PdGATL1.1*-complemented *parvus*, *PdGATL1.2*-complemented *parvus*, and *parvus*, respectively.
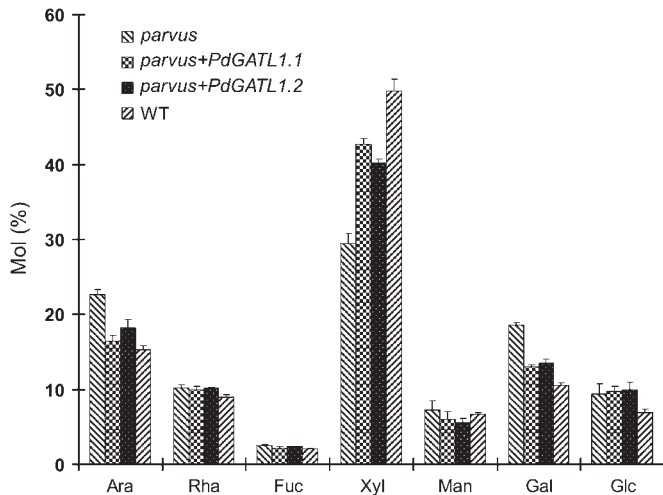
Figure 6. Monosaccharide Composition of Cell Walls Isolated from the Stems of *parvus*, *parvus* Complemented with *PdGATL1.1*, *parvus* Complemented with *PdGATL1.2*, and Wild-Type Plants.

Cell walls were prepared from stems of 8-week-old plants and their glycosyl compositions determined as described in Methods. Data are means (Mol %) $\pm$ SE of analyses carried out on three biological replicates and each replicate represents cell walls isolated from five transgenic plants.

Figure 7. Immunofluorescent Labeling of Transverse Sections of Wild-Type, *parvus* + *PdGATL1.1*, *parvus* + *PdGATL1.2*, and *parvus* Stems and Hypocotyls.

Labeling was carried out on 250-nm-thick transverse sections taken from stem (A-H) and hypocotyls (I-P) tissues of 7-week-old w.t. (column 1), *parvus* + *PdGATL1.1* (column 2), *parvus* + *PdGATL1.2* (column 3), and *parvus* (column 4) plants. Antibodies used for labeling are indicated in the figure. Arrows indicate fibers and xylem vessels. if, interfascicular fiber; xy, xylem; sx, secondary xylem. Bars = 50 μm.

arabinoxylan (McCartney et al., 2005). Immunolabeling of cross-sections of w.t. stems and hypocotyls with LM10 and LM11 showed strong antibody binding to the walls of interfascicular fibers and xylem cells (Figure 7), both of which have abundant xylan in their secondary cell walls (York and O'Neill, 2008). Less labeling with these antibodies was observed in *parvus/gatl1* stems, although the overall pattern of labeling was unchanged from w.t. plants. In *PdGATL1.1* or *PdGATL1.2* complemented *parvus/gatl1*, the levels of labeling with LM10 and LM11 were restored to w.t. levels in the walls of both interfascicular fibers and xylem cells (Figure 7). Control sections in which the primary antibodies were omitted showed little, if any, fluorescence (data not shown). These results show that both PdGATL1.1 and PdGATL1.2 can perform a similar biochemical function as PARVUS/GATL1 and largely complement the xylan deficiency of the *parvus* mutant.

DISCUSSION

Two close homologs of the *Arabidopsis thaliana PARVUS/ GATL1* gene, named *GATL1.1* and *GATL1.2*, were identified in a BLAST search of the *Populus trichocarpa* genome, and subsequently cloned from the closely related *P. deltoides*. Their predicted protein products share 82 and 81% overall amino acid identity with PARVUS/AtGATL1, respectively.

PARVUS/AtGATL1 has been suggested to play a role in xylan synthesis in *Arabidopsis* (Brown et al., 2007; Lee et al., 2007). We have demonstrated that overexpression of either *PdGATL1.1* or *PdGATL1.2* can compensate all of the morphological changes and most of the cell wall defects caused by
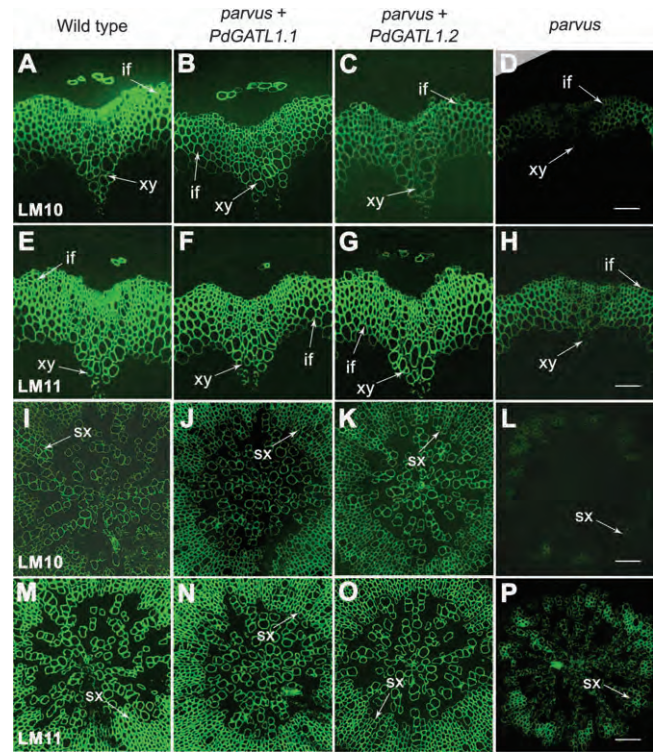
the *parvus* mutation in *Arabidopsis*. It is interesting to note that although the xylose deficiency in cell walls of the mutant was only partially rescued by expression of the poplar orthologs, the patterns and intensity of xylan immunolabeling in the complemented plants are comparable with those observed in w.t. plants. This phenomenon was also observed in *PoGT43B* complemented *irx9* plants, in which the xylose defect was partially rescued, but the thickness of secondary walls in fibers and vessels was restored to w.t. level (Zhou et al., 2007). These results provide strong evidence that these two poplar genes are functional orthologs of *PARVUS/AtGATL1* and suggest that genes involved in secondary wall formation are, at least in part, functionally conserved between the herbaceous plant, *Arabidopsis*, and the woody species, poplar.

Quantitative RT–PCR analysis showed that *PdGATL1.1* is strongly expressed in poplar xylem cells. *PARVUS* was also found to be highly expressed in interfascicular fibers and xylem cells in *Arabidopsis* and has been implicated in the synthesis of secondary wall xylan (Brown et al., 2007; Lee et al., 2007). The observed expression patterns for *PdGATL1.1* and *AtGATL1*

in poplar and *Arabidopsis*, respectively, are consistent with a role for GATL1 in xylan synthesis. The similar expression patterns further support the functional conservation of these genes between *Arabidopsis* and *Populus*.

Although *PdGATL1.1* and *PdGATL1.2* share 93% identity in amino acid sequence, the different expression patterns of these two genes in *Populus* tissues suggest that they do not play identical roles in cell wall biosynthesis in poplar. *PdGATL1.2* shows a much lower level of transcription than *PdGATL1.1* and its expression is fairly uniform in cortex, phloem, xylem, shoot tip, and leaf, while *PdGATL1.1* is highly expressed only in xylem tissue. Such a differential pattern of expression between gene pairs is common in *Populus* wood-forming organs. About 14% of the duplicated genes were reported to display differential expression in nodes and internodes of *Populus* (Tuskan et al., 2006). According to the duplication–degeneration–complementation (DDC) model proposed by Force et al. (1999), most duplicated genes accumulate degenerative mutations for some time after the duplication event and then undergo functional specialization by complementary partitioning of the functions of the ancestral gene. In other words, preservation of duplicated genes is through complementary sub-functionalization of the progenitor gene's functions rather than through the evolution of new functions (Force et al., 1999). The differences in gene expression patterns observed for *PdGATL1.1* and *PdGATL1.2* suggest that this type of sub-functionalization has occurred for these two poplar genes, whereas, in *Arabidopsis*, all *GATL1* functions are carried out by a single gene.

The haploid genome size of *P. trichocarpa* is around 485 Mb, which is similar in size to rice, about four times larger than *Arabidopsis*, and 40 times smaller than pine (Brunner et al., 2004a). A total of 45 555 gene models have been predicted in *P. trichocarpa* to date (Tuskan et al., 2006). Among the predicted gene models, 1603 are carbohydrate-active enzymes (CAZymes; http://www.cazy.org/ (Cantarel et al., 2009)), which is 1.6 times the number identified in the *Arabidopsis* genome. Indeed, poplar has the largest number of CAZyme genes observed among the fully sequenced plant genomes (Geisler-Lee et al., 2006). It was also found that the number of lignin biosynthesis-related genes in *Populus* is larger than in *Arabidopsis*, and some of these genes occur in duplicate pairs relative to single copies in *Arabidopsis* (Tuskan et al., 2006), suggesting a greater need for the expression of these genes in poplar during the massive commitment to cell wall biosynthesis that occurs during wood formation. Alternatively, it could reflect pressure for sub-functionalization.

Sub-cellular localization experiments showed that the PdGATL1.1 and PdGATL1.2 proteins are located in the secretory pathway, including ER and Golgi. Current models of cell wall synthesis propose that non-cellulosic polysaccharides are synthesized in the Golgi and transported to the cell wall in Golgi-derived vesicles (Turner et al., 2007). For example, there is considerable evidence that the glycosyltransferases that are involved in xylan synthesis in *Arabidopsis*, including IRX7, IRX8, and IRX9, are localized to the Golgi (Zhong et al., 2005; Peña et al., 2007), consistent with previous findings of the site for xylan synthesis in French bean (Gregory et al., 2002). Our present work showed that although PdGATL1.1 and PdGATL1.2 do localize to the Golgi, they are also present in the ER. Although a Golgi retention signal has not yet been identified, all glycosyltransferases characterized thus far have a similar domain structure. They are all type II transmembrane proteins that contain a short N-terminal cytosolic region, a single membrane-spanning domain and a large luminal domain that contains the catalytic site. In general, the membrane-spanning and luminal domains appear to be most important for robust localization of Golgi enzymes (Colley, 1997; Munro, 1998). Since no transmembrane domain appears to be present in PdGATL1.1 and PdGATL1.2, these two proteins may need to form a complex with other membrane-anchored components in order to be targeted to the endomembrane system. In *N. benthamiana* cells, the presence of PdGATL1.1 and PdGATL1.2 in the ER might occur because of the high level of expression of the *PdGATL1.1* and *PdGATL1.2* genes such that there are insufficient amounts of partner components available to form functional complexes and thus some PdGATL1.1 and PdGATL1.2 are left in the ER. Alternatively, overexpression of a protein might saturate a trafficking pathway resulting in the accumulation of a fusion protein in an earlier endomembrane compartment (Sparkes et al., 2006). However, we used bacterial inoculum levels that are on the low end of those reported in the literature for these kinds of studies (Hanton et al., 2005; Renna et al., 2005; Hanton et al., 2009) to avoid pathway saturation, and the marker proteins expressed under the same promoter showed no unexpected localization patterns in our studies.

Previous studies using carrot protoplasts as the heterologous expression system showed that the PARVUS/GATL1 protein in *Arabidopsis* is located only in the ER (Lee et al., 2007). The differences in sub-cellular localization of GATL1 proteins in these two studies might be due to the absence of partnering components in carrot protoplasts, given that no cell wall is present in protoplasts, whereas such partners appear available in tobacco leaf cells that do have walls. Direct immunolocalization of GATL1 protein using specific antibodies would resolve uncertainties about the sub-cellular localization of GATL1, although this approach may be problematic, given the low expression levels of most cell wall-related glycosyltransferases. Furthermore, the high degree of sequence similarity amongst GATL proteins may preclude the generation of GATL1-specific antibodies. Identification of proteins that interact with GATL1 to form synthetic complexes will be necessary to more clearly explain how the GATL1 protein is retained within the endomembrane compartment, rather than being transported to the apoplast, as would be expected for proteins that carry no targeting signals (Rojo and Denecke, 2008).

In conclusion, we have shown that *PdGATL1.1* and *PdGATL1.2* are functional orthologs of *AtGATL1* and that the corresponding proteins are targeted to the secretory pathway in plant cells. Further, we have provided evidence that the two poplar genes

have become functionally specialized since the duplication event that gave rise to these two paralogous genes. Lastly, the expression pattern observed for *PdGATL1.1* is consistent with an involvement of this gene in the synthesis of secondary wall polysaccharides (e.g. xylan) that occurs in developing xylem. The results of this study provide further evidence that *Arabidopsis* is a suitable experimental system for functional studies of genes involved in wood formation in trees.

METHODS

Bioinformatic Analyses of GATL Protein Sequences

Protein sequences in *Populus trichocarpa* similar to PARVUS/AtGATL1 were identified by a BLAST search (http://blast.ncbi.nlm.nih.gov/Blast.cgi) of the *P. trichocarpa* genome (www.jgi.doe.gov/poplar). The *P. trichocarpa* sequences identified from the BLAST search were aligned with all 10 AtGATL protein sequences using MAFFT v6.603 (Katoh et al., 2005) and the resulting alignment was used to perform maximum likelihood phylogeny reconstruction using PhyML v2.4.4 (Guindon and Gascuel, 2003). PhyML analyses were conducted with the JTT model, 1000 replicates of bootstrap analyses, estimated proportion of invariable sites (considering a fraction of amino acids to be invariable during the evolution), four rate categories (assign each site a probability to belong to given evolutionary rate categories), estimated gamma distribution parameter, and optimized starting BIONJ tree. The resulting tree was visualized using Treeview (Page, 2009) and the figure generated using PowerPoint™.

Plant Material

Arabidopsis plants were grown on soil in controlled-environment cabinets under a 16-h light/8-h dark cycle at 19°C during the light period and 15°C during the dark period. The light intensity was 120 μmol m^{-2} s^{-1}, and the relative humidity was maintained at 70%. *Populus deltoides* saplings were obtained from Arborgen LLC (Summerville, SC) and were grown on soil in a greenhouse and watered every day and fertilized every 2 months. Approximately 1-year-old plants were used to collect different tissues (see below).

Screening of Homozygous Plants with T-DNA Insertion

Identification of homozygous plants with T-DNA insertions in At1g19300 (*parvus-3*, Salk_045368) was performed as described by Brown et al. (2007). Briefly, T-DNA insertions were identified using the flanking primers (LP and RP) generated by the SIGnal T-DNA verification primer design website (http://signal.salk.edu/tdnaprimers.html) and primers from the T-DNA left border LBa1 (5′-GCGTGGACCGCTTGCTGCAACT-3′) and LBb1 (5′-TCAAACAGGATTTTCGCCTGCT-3′).

Quantitative Real-Time PCR

Cortex, developing phloem, and developing xylem were harvested from the bottom stems by sequential peeling essen-

tially as described (Suzuki et al., 2006). In addition, young shoot tips (first to third internodes), leaves (from the fourth to the sixth internode), and fine root tissues were also harvested. All tissues were frozen immediately in liquid nitrogen and stored at –80°C until use. Total RNA was isolated using RNeasy plant mini kits (Qiagen) and then treated with RNase-free DNase (Qiagen) to remove contaminating genomic DNA. 1 μg of total RNA was reverse-transcribed using Superscript® III Reverse Transcriptase (Invitrogen). Quantitative real-time PCR (qRT–PCR) was performed in 20 μl of reaction mixture, composed of 1 μl of a given cDNA, 10 μl master mix IQ™ SYBR® Green Supermix (Bio-Rad), 0.4 μl each primers (10 μM), and 8.2 μl nuclease-free water. Each reaction was repeated three times using cDNAs generated from independently isolated RNA preparations. Amplifications were performed using an iCycler iQ System (Bio-Rad) under the following conditions: initial polymerase activation: 95°C, 4 min; then 45 cycles of 10 s at 95°C and 30 s at 55.2°C.

The primers to amplify the transcripts of the two genes were as follows: *PdGATL1.1* (forward, 5′-GGAGTGGATGGAACTACAGA-3′; reverse, 5′-GCAAGAGACTAACAGGACCA-3′), *PdGATL1.2* (forward, 5′-GCCTAGACTGATCCACAAAC-3′; reverse, 5′-CTGAGTCG-GAGTCTATTCCA-3′). In addition, two primers (forward, 5′-GTTGATTTTTGCTGGGAAGC-3′; reverse, 5′-GATCTTGGCCTTCA-CGTTGT-3′) to amplify the ubiquitin (BU879229) (Brunner et al., 2004b) transcript were also designed as an internal standard for quantification. A melting curve was produced at the end of every experiment to ensure that only single products were formed. The reliability of primers was also examined by running the products on an agrose gel to ensure that only a single band was present. The relative expression level was calculated by using the comparative C$_T$ (threshold cycle value) (Livak and Schmittgen et al., 2001). The expression level of ubiquitin was measured and used as a point of reference, being a housekeeping gene (Rajinikanth et al., 2007).

Mutant Complementation Analysis

The *PdGATL1.1* and *PdGATL1.2* cDNAs were isolated by RT–PCR from *Populus deltoides* developing xylem cDNAs. Gene-specific primers were designed based on the *Populus trichocarpa* sequences (5′-CTAGCCACCTATTTTTAATTTCCC-3′ and 5′- CGAT-CCTTGAAACTTGACATC-3′ for *PdGATL1.1*, and 5′-CTCCATAGCC AAGAGCTACATGTC-3′ and 5′-CACTAACATCTTCGAATCCATGA-GAG-3′ for *PdGATL1.2*). The amplified fragments were ligated into T-easy vector and sequenced using a dye-based cycle sequencing kit (Applied Biosystems, Foster City, CA, USA). The sequences obtained were used for designing the primers used for cloning of the open reading frames that is described below.

For complementation analysis, the plant transformation vector pCAMBIA (CAMBIA) was used for the generation of transformed plants and the full-length *PdGATL1.1* and *PdGATL1.2* open reading frames were PCR-amplified from the fragments sequenced above, respectively, with PCR primers as follows: *PdGATL1.1* (PdGATL1.1OV-F) 5′-TATATGG-TACCCTAGCCACCTATTTTTAATTTCCC-3′ and (PdGATL1.1OV-R)

5′-TATACTCTAGACGATCCTTGAAACTTGACATC-3′; *PdGATL1.2* (PdGATL1.2OV-F) 5′-AATTGGGTACCCTCCATAGCCAAGAGCTA-CATGTC-3′ and (PdGATL1.2OV-R) 5′-TTTACTCTAGACACTAA-CATCTTCGAATCCATGAGAG-3′. The DNA fragments were each inserted between the CaMV 35S promoter and the nopa-line synthase 3′-terminator in separate pCAMBIA vectors. The constructs were introduced into *Arabidopsis parvus/gatl1* mutant plants by using the *Agrobacterium*-mediated floral dip method (Clough and Bent, 1998). Transgenic plants were selected on hygromycin, and homozygous lines were identi-fied by PCR and the first generation of transgenic plants was used for morphological and anatomical analyses.

Topological Analysis of GATL1 Proteins

The following websites were used for topological analysis of the PdGATL1 proteins: SOSUI Classification and Secondary Structure Prediction of Membrane Proteins (http://bp.nuap.nagoya-u.ac.jp/sosui/), TMHMM server version 2.0 (www.cbs.dtu.dk/services/TMHMM/), and PSORT (http://psort.ims.u-tokyo.ac.jp/form.html/).

Sub-Cellular Localization of PdGATL1.1 and PdGATL1.2

The *PdGATL1.1* and *PdGATL1.2* coding regions were cloned in-frame with an enhanced yellow fluorescent protein (EYFP) gene under the control of the 35S promoter in a pCAMBIA-based binary vector (Pattathil et al., 2005) to generate the fu-sion constructs 35S-*PdGATL1.1-EYFP* and 35S-*PdGATL1.2-EYFP*. The *PdGATL1.1* coding region was amplified with the primers PdGATL1.1-F (5′-AATTATCATGAGCATGCTCATGCCTAGACTGA-TCCG-3′) and PdGATL1.1-R (5′-AATTAGTCGACCAAGAATC-CAAGGCGAATGGAGTC-3′) and the *PdGATL1.2* coding region was amplified with the primers PdGATL1.2-F (5′-AATTATCAT-GAACATGCTTATGCCTAGACTGATCC-3′) and PdGATL1.2-R (5′-AATTAGTCGACCAACAATCCAAGGCAAATGGAGTC-3′) us-ing xylem-derived cDNA as the template. The *PdGATL1* con-structs were sequenced and then transformed individually into *Agrobacterium tumefaciens* GV3101 strain. The constructs were individually co-transformed into fully expanded leaf of *Nicotiana benthamiana* plants (∼8-week-old seedlings grown at 22°C) together with the enhanced cyan fluorescent protein (ECFP)-tagged markers specific to either the Golgi or the endo-plasmic reticulum (ER) compartments. Golgi localization was based on the cytoplasmic tail and transmembrane domain (first 49 aa) of soybean α-1,2-mannosidase I (GmMan1) (Saint-Jore-Dupas et al., 2006; Nelson et al., 2007) (Gmct–ECFP). The ER marker, ECFP–WAK2–HDEL, was created by combining the signal peptide of *Arabidopsis thaliana* wall-associated ki-nase 2 (AtWAK2) (He et al., 1999) at the N-terminus of the fu-sion protein and the ER retention signal His–Asp–Glu–Leu (HDEL) at its C-terminus (Nelson et al., 2007). Co-transformation was done as described previously (Johansen and Carrington, 2001), using three different bacterial densities (OD_{600} = 0.05, 0.3, and 3) as suggested by the Brandizzi group (Hanton et al., 2005; Renna et al., 2005; Hanton et al., 2009). The reported localization results are from the plants with the lowest bacterial

innoculum, but similar localization patterns were observed for all three bacterial densities. Three or four days post-infection, the injected area (∼2.5 cm radius) was cut and subsequently ex-amined for yellow and cyan fluorescent signals using a Leica TCs SP2 confocal microscope (Leica Microsystems, Heidelberg, Germany). For the co-localization studies, excitation lines of an argon ion laser of 458 nm for CFP and 514 nm for EYFP were used alternately with line switching using the line-sequencing scanning facility of the microscope. Fluorescence was detected using a 475–525-nm bandpass filter for CFP and a 530–590-nm bandpass filter for EYFP. Images were saved and processed with Adobe Photoshop version 7.0 (Adobe Systems, San Jose, CA).

Microscopic Investigations of Stem and Hypocotyl Structure

Stems and hypocotyls from 8-week-old transgenic *Arabidopsis* plants were fixed in 2.5% glutaraldehyde buffered with 0.05 M phosphate buffer (pH 6.8) at 4°C for 24 h. After fixa-tion, the tissues were dehydrated using an ethanol series and embedded in LR White resin (Ted Pella Inc., Redding, CA) as described (Freshour et al., 1996). Sections (250 nm thick) were cut using a Reichert-Jung Ultracut E ultra microtome (Reichert-Jung, Wien, Austria) and stained with toluidine blue for light microscopy, carried out on an Eclipse80i microscope (Nikon, Melville, NY). Images were captured with a Nikon DS-Ril camera head (Nikon, Melville, NY) using NIS-Elements Basic Research software and images were assembled using Adobe Photoshop 7.0.

Immunolocalization of Xylan

For detection of xylan, sections (250 nm thick) of stems and hypocotyls prepared as described above were incubated with the LM10 and LM11 monoclonal antibodies, which recog-nize glucuronoxylan (PlantProbes; www.plantprobes.net) (McCartney et al., 2005), and then with 1:100 diluted goat anti-rat-fluorescein isothiocyanate-conjugated secondary antibodies (Invitrogen). Negative controls were carried out in the absence of primary antibody. The fluorescence-labeled sections were observed using the Nikon Eclipse80i microscope equipped with epifluorescence optics and photographed at identical exposure times for all sections as described above.

Cell Wall Isolation and Extraction

Cell walls were prepared as alcohol-insoluble residues as described previously (Persson et al., 2007). In brief, stems from 10-week-old *Arabidopsis* plants were harvested on ice, flash-frozen in liquid nitrogen, and ground to a fine powder with a mortar and pestle. The ground material was extracted over a sintered glass funnel (Kimax 60M) under vacuum sequen-tially with 2 vol. of 100 mL of ice-cold 80% (v/v) ethanol, 100% ethanol, chloroform:methanol (1:1; v/v), and 100% ace-tone. Starch was removed from the walls by treatment with Type-I porcine α-amylase (Sigma-Aldrich; 47 units/100 mg cell wall) in 100 mM ammonium formate for 48 h at 25°C with ro-tation. De-starched walls were centrifuged, washed twice with

sterile water, twice with 100% acetone, and air dried. Sugar composition analyses were carried out on three independently prepared cell wall preparations as described below.

Monosaccharide Analyses

Each sample (1–2 mg) was hydrolyzed with 2 M TFA containing 20 μg of *myo*-inositol (internal standard) for 90 min at 120°C, after which the acid was removed by drying under an air stream and the samples washed twice with isopropanol. Reduction was performed by incubation for 2 h in sodium borohydride (10 mg ml^{-1}) dissolved in 1 M ammonium hydroxide. Samples were neutralized with glacial acetic acid, and methanol:acetic acid (9:1, v/v) was added before drying the samples and washing them with methanol. *O*-acetylation was performed by adding acetic anhydride and concentrated TFA for 10 min at 50°C. The samples were washed with isopropanol and dried (repeated twice). Sodium carbonate (0.2 M) and dichloromethane were added, and the samples were vortexed and centrifuged before removing the aqueous phase. Water was added, and the samples were vortexed and briefly centrifuged. The aqueous layer was removed, and the procedure was repeated. The organic phase was transferred, and the sample was concentrated to 100 μl. The alditol acetates were separated by gas-liquid chromatography on an Agilent 6890N (Wilmington, DE, USA) equipped with a 30 m × 0.25 mm (i.d.) silica capillary column DB 225 (Alltech Assoc., Deerfield, IL, USA). The temperature was held at 80°C for 1 min upon injection, then programmed from 80 to 170°C at 25°C min^{-1}, then to 240°C at 5°C min^{-1}, with a 6-min hold at the upper temperature.

Accession Numbers

Sequence data for PdGATL1.1 and PdGATL1.2 described in this article can be found in the GenBank data library under accession numbers GQ464114 and GQ464115.

REFERENCES

Andersson-Gunnerås, S., Mellerowicz, E.J., Love, J., Segerman, B., Ohmiya, Y., Coutinho, P.M., Nilsson, P., Henrissat, B., Moritz, T., and Sundberg, B. (2006). Biosynthesis of cellulose-enriched tension wood in *Populus*: global analysis of transcripts and metabolites identifies biochemical and developmental regulators in secondary wall biosynthesis. Plant J. **45**, 144–165.

Aspeborg, H., et al. (2005). Carbohydrate-active enzymes involved in the secondary cell wall biogenesis in hybrid aspen. Plant Physiol. **137**, 983–997.

Bevan, M.W., and Franssen, M.C.R. (2006). Investing in green and white biotech. Nature Biotechnology. **24**, 765–767.

Brown, D.M., Goubet, F., Vicky, W.W., Goodacre, R., Stephens, E., Dupree, P., and Turner, S.R. (2007). Comparison of five xylan synthesis mutants reveals new insight into the mechanisms of xylan synthesis. Plant J. **52**, 1154–1168.

Brown, D.M., Zhang, Z., Stephens, E., Dupree, P., and Turner, S.R. (2009). Characterization of IRX10 and IRX10-like reveals an essential role in glucuronoxylan biosynthesis in *Arabidopsis*. Plant J. **57**, 732–746.

Brunner, A.M., Busov, V.B., and Strauss, S.H. (2004a). Poplar genome sequence: functional genomics in an ecologically dominant plant species. Trends Plant Sci. **9**, 49–56.

Brunner, A.M., Yakovlev, I.A., and Strauss, S.H. (2004b). Validating internal controls for quantitative plant gene expression studies. BMC Plant Biol. **4**, 14–20.

Cantarel, B.L., Coutinho, P.M., Rancurel, C., Bernard, T., Lombard, V., and Henrissat, B. (2009). The Carbohydrate-Active EnZymes database (CAZy): an expert resource for Glycogenomics. Nucleic Acids Res. **37**, D233–D238.

Chaffey, N., Cholewa, E., Regan, S., and Sundberg, B. (2002). Secondary xylem development in *Arabidopsis*: a model for wood formation. Physiol. Plant. **114**, 594–600.

Clough, S.J., and Bent, A.F. (1998). Floral dip: a simplified method for *Agrobacterium*-mediated transformation of *Arabidopsis thaliana*. Plant J. **16**, 735–743.

Colley, K.J. (1997). Golgi localization of glycosyltransferases: more questions than answers. Glycobiology. **7**, 1–13.

Ebringerová, A., Hromádková, Z., and Heinze, T. (2005). Hemicellulose. Advances in Polymer Science. **186**, 1–67.

Force, A., Lynch, M., Pickett, F.B., Amores, A., Yan, Y.-l., and Postlethwait, J. (1999). Preservation of duplicate genes by complementary, degenerate mutations. Genetics. **151**, 1531–1545.

Freshour, G., Clay, R.P., Fuller, M.S., Albersheim, P., Darvill, A.G., and Hahn, M.G. (1996). Developmental and tissue-specific structural alterations of the cell-wall polysaccharides of *Arabidopsis thaliana* roots. Plant Physiol. **110**, 1413–1429.

Geisler-Lee, J., et al. (2006). Poplar carbohydrate-active enzymes: gene identification and expression analyses. Plant Physiol. **140**, 946–962.

Gregory, A.C.E., Smith, C., Kerry, M.E., Wheatley, E.R., and Bolwell, G.P. (2002). Comparative subcellular immunolocation of polypeptides associated with xylan and callose synthases in French bean (*Phaseolus vulgaris*) during secondary wall formation. Phytochemistry. **59**, 249–259.

Guindon, S., and Gascuel, O. (2003). A simple, fast, and accurate algorithm to estimate large phylogenies by maximum likelihood. Systematic Biology. **52**, 696–704.

Hanton, S.L., Matheson, L.A., Chatre, L., and Brandizzi, F. (2009). Dynamic organization of COPII coat proteins at endoplasmic reticulum export sites in plant cells. Plant J. **57**, 963–974.

Hanton, S.L., Renna, L., Bortolotti, L.E., Chatre, L., Stefano, G., and Brandizzi, F. (2005). Diacidic motifs influence the export of transmembrane proteins from the endoplasmic reticulum in plant cells. Plant Cell. **17,** 3081–3093.

He, Z.H., Cheeseman, I., He, D.Z., and Kohorn, B.D. (1999). A cluster of five cell wall-associated receptor kinase genes, *Wak1-5*, are expressed in specific organs of *Arabidopsis*. Plant Mol. Biol. **39,** 1189–1196.

Johansen, L.K., and Carrington, J.C. (2001). Silencing on the spot: induction and suppression of RNA silencing in the *Agrobacterium*-mediated transient expression system. Plant Physiol. **126,** 930–938.

Katoh, K., Kuma, K., Toh, H., and Miyata, T. (2005). MAFFT version 5: improvement in accuracy of multiple sequence alignment. Nucl. Acids Res. **33,** 511–518.

Ko, J.-H., and Han, K.-H. (2004). *Arabidopsis* whole-transcriptome profiling defines the features of coordinated regulations that occur during secondary growth. Plant Mol. Biol. **55,** 433–453.

Lao, N.T., Long, D., Kiang, S., Coupland, G., Shoue, D.A., Carpita, N.C., and Kavanagh, T.A. (2003). Mutation of a family 8 glycosyltransferase gene alters cell wall carbohydrate composition and causes a humidity-sensitive semi-sterile dwarf phenotype in *Arabidopsis*. Plant Mol. Biol. **53,** 687–701.

Lee, C., Zhong, R., Richardson, E.A., Himmelsbach, D.S., McPhail, B.T., and Ye, Z.-H. (2007). The *PARVUS* gene is expressed in cells undergoing secondary wall thickening and is essential for glucuronoxylan biosynthesis. Plant Cell Physiol. **48,** 1659–1672.

Livak, K.J., and Schmittgen, T.D. (2001). Analysis of relative gene expression data using real time quantitative PCR and the $2^{-\triangle\triangle C}{}_T$ method. Methods. **25,** 402–408.

McCartney, L., Marcus, S.E., and Knox, J.P. (2005). Monoclonal antibodies to plant cell wall xylans and arabinoxylans. J. Histochem. Cytochem. **53,** 543–546.

Mellerowicz, E.J., and Sundberg, B. (2008). Wood cell walls: biosynthesis, developmental dynamics and their implications for wood properties. Curr. Opin. Plant Biol. **11,** 293–300.

Mohnen, D. (2008). Pectin structure and biosynthesis. Curr. Opin. Plant Biol. **11,** 266–277.

Munro, S. (1998). Localization of proteins to the Golgi apparatus. Trends Cell Biol. **8,** 11–15.

Nelson, B.K., Cai, X., and Nebenführ, A. (2007). A multicolored set of *in vivo* organelle markers for co-localization studies in *Arabidopsis* and other plants. Plant J. **51,** 1126–1136.

Page, R.D.M. (2009). TREEVIEW: an application to display phylogenetic trees on personal computers. Comput. Appl. Biosci. **1996,** 357–358.

Pattathil, S., Harper, A.D., and Bar-Peled, M. (2005). Biosynthesis of UDP-xylose: characterization of membrane-bound AtUxs2. Planta. **221,** 538–548.

Peña, M.J., Zhong, R., Zhou, G.-K., Richardson, E.A., O'Neill, M.A., Darvill, A.G., York, W.S., and Ye, Z.-H. (2007). *Arabidopsis irregular xylem8* and *irregular xylem9*: implications for the complexity of glucuronoxylan biosynthesis. Plant Cell. **19,** 549–563.

Persson, S., Caffall, K.H., Freshour, G., Hilley, M.T., Bauer, S., Poindexter, P., Hahn, M.G., Mohnen, D., and Somerville, C. (2007). The *Arabidopsis irregular xylem8* mutant is deficient in glucuronoxylan and homogalacturonan, which are essential for secondary cell wall integrity. Plant Cell. **19,** 237–255.

Rajinikanth, M., Harding, S.A., and Tsai, C.-J. (2007). The glycine decarboxylase complex multienzyme family in *Populus*. J. Exp. Bot. **58,** 1761–1770.

Renna, L., Hanton, S.L., Stefano, G., Bortolotti, L., Misra, V., and Brandizzi, F. (2005). Identification and characterization of AtCASP, a plant transmembrane Golgi matrix protein. Plant Mol. Biol. **58,** 109–122.

Rojo, E., and Denecke, J. (2008). What is moving in the secretory pathway of plants? Plant Physiol. **147,** 1493–1503.

Saint-Jore-Dupas, C., Nebenfuhr, A., Boulaflous, A., Follet-Gueye, M.L., Plasson, C., Hawes, C., Driouich, A., Faye, L., and Gomord, V. (2006). Plant N-glycan processing enzymes employ different targeting mechanisms for their spatial arrangement along the secretory pathway. Plant Cell. **18,** 3182–3200.

Shao, M., Zheng, H., Hu, Y., Liu, D., Jang, J.-C., Ma, H., and Huang, H. (2004). The *GAOLAOZHUANGREN1* gene encodes a putative glycosyltransferase that is critical for normal development and carbohydrate metabolism. Plant Cell Physiol. **45,** 1453–1460.

Simson, B.W., and Timell, T.E. (1978). Polysaccharides in cambial tissues of *Populus tremuloides* and *Tilia americana*. III. Isolation and constitution of an arabinogalactan. Cellul. Chem. Technol. **12,** 63–77.

Sparkes, I.A., Runions, J., Kearns, A., and Hawes, C. (2006). Rapid, transient expression of fluorescent fusion proteins in tobacco plants and generation of stably transformed plants. Nature Protocols. **1,** 2019–2025.

Sterling, J.D., Atmodjo, M.A., Inwood, S.E., Kumar Kolli, V.S., Quigley, H.F., Hahn, M.G., and Mohnen, D. (2006). Functional identification of an *Arabidopsis* pectin biosynthetic homogalacturonan galacturonosyltransferase. Proc. Natl Acad. Sci. USA. **103,** 5236–5241.

Suzuki, S., Li, L., Sun, Y.-H., and Chiang, V.L. (2006). The cellulose synthase gene superfamily and biochemical functions of xylem-specific cellulose synthase-like genes in *Populus trichocarpa*. Plant Physiol. **142,** 1233–1245.

Turner, S., Gallois, P., and Brown, D. (2007). Tracheary element differentiation. Ann. Rev. Plant Biol. **58,** 407–433.

Tuskan, G.A., et al. (2006). The genome of black cottonwood, *Populus trichocarpa* (Torr. & Gray). Science. **313,** 1596–1604.

Wu, A.-M., Rihouey, C., Seveno, M., Hörnblad, E., Singh, S.K., Matsunaga, T., Ishii, T., Lerouge, P., and Marchant, A. (2009). The *Arabidopsis* IRX10 and IRX10-LIKE glycosyltransferases are critical for glucuronoxylan biosynthesis during secondary cell wall formation. Plant J. **57,** 718–731.

York, W.S., and O'Neill, M.A. (2008). Biochemical control of xylan biosynthesis: which end is up? Curr. Opin. Plant Biol. **11,** 258–265.

Zhong, R., Peña, M.J., Zhou, G.-K., Nairn, C.J., Wood-Jones, A., Richardson, E.A., Morrison, W.H.III, Darvill, A.G., York, W.S., and Ye, Z.-H. (2005). *Arabidopsis Fragile Fiber8*, which encodes a putative glucuronyltransferase, is essential for normal secondary wall synthesis. Plant Cell. **17,** 3390–3408.

Zhou, G., Zhong, R., Richardson, E.A., Morrison, W.H., Nairn, C.J., Wood-Jones, A., and Ye, Z.-H. (2006). The poplar glycosyltransferase GT47C is functionally conserved with *Arabidopsis Fragile fiber8*. Plant Cell Physiol. **47,** 1229–1240.

Zhou, G.-K., Zhong, R., Himmelsbach, D.S., McPhail, B.T., and Ye, Z.-H. (2007). Molecular characterization of PoGT8D and PoGT43B, two secondary wall-associated glycosyltransferases in poplar. Plant Cell Physiol. **48,** 689–699.